http://ansinet.com/itj

ITJ

ISSN 1812-5638

INFORMATION TECHNOLOGY JOURNAL

ANSInet
Asian Network for Scientific Information
308 Lasani Town, Sargodha Road, Faisalabad - Pakistan

Information Technology Journal 11 (2): 289-293, 2012
ISSN 1812-5638 / DOI: 10.3923/itj.2012.289.293

Camera Calibration for Direct-Reading Water-Meter Based on Round Feature

Li Xue-Cong, Wang Ren-Huang and Liu Hong-Jiang
No. 100 Waihuan Xi Road, Guangzhou Higher Education Mega Center,
Panyu District, Guangzhou, People's Republic of China
Faculty of Automation, Guangdong University of Technology, 510006, China

Abstract: Familiar methods of camera calibration are very hard to be applied to direct-reading water-meter because the camera on water-meter is limited by operating space and fixing condition. In this study, a new calibration method was proposed by utilizing plenty of round features on water-meter surface. Firstly, the center of round feature was roughly located by template matching. Secondly, the region around round feature was locked. Thirdly, the edge of round feature was extracted by Canny operator and the center of round feature was accurately located according to these edges. Lastly, calibration was carried out with these accurate centers and asymmetric error was corrected. Experimental results showed that the method proposed in this study was practical to calibration for camera fixed on direct-reading water-meter.

Key words: Camera calibration, template matching, region locked, edge detection, asymmetric error, rough location

INTRODUCTION

Data-reading has become easy when camera was used in water-meter. These water-meters were named direct-reading water-meters (Hovany, 2011). Camera collection and image processing technology has been widely used in reading datum of these meters. Camera calibration is very important to the whole course (Pu *et al*., 2011). Precision of image processing is decided by calibration result and accuracy of datum-reading is also influenced. There are many good methods for camera calibration such as traditional calibration, self-calibration and calibration based on active vision (Zhao-Zheng and Qi-Mei, 2010). Three-dimensions calibration body or two-dimensions calibration template is used in traditional calibration and their size should be known. When relation between points in calibration body and homologous points in image is established, intrinsic parameters and extrinsic parameters of camera can be obtained. A two-step calibration method was proposed, where high-precision solid calibration body was used. This method has a good calibration result but calibration body is hard be machined (Tsai, 1987). A simple calibration method was proposed, where planar calibration template was used. Zhang improved calibration algorithm not using high-precision solid calibration body (Zhang, 2000). Restriction information in scene is used in self-calibration. Advantage of self-calibration is agile and on-line and disadvantage is not robust (Seo *et al*., 2011; Espuny and Gil, 2011). Camera should accomplish some movements if it was calibrated based on active vision. A calibration method was proposed by rotating camera repeatedly (Hartley, 1999). However, these calibration methods are very hard to be applied to direct-reading water-meter because the camera on water-meter is limited by operating space and fixing condition. So, a new calibration method was proposed by utilizing plenty of round features on water-meter surface in this study.

MATERIALS AND METHODS

Round feature on the surface of water-meter: There are plenty of round features on the surface of water-meter. These rounds can be used in camera calibration. A water-meter image is shown as Fig. 1.

From Fig. 1, it can be seen that the region around pointers and the whole profile are all circles. The centers of circles are collected as reliable datum using in many calibration methods. If the centers of round features on the surface of water-meter could be obtained accurately, camera fixed on the water-meter would be calibrated.

Rough location of round center: In order to obtain accurate coordinate of every round center, round center was first located approximately. In this course, pointer was taken as template and template matching was carried out. All operations are shown as Fig. 2.

Corresponding Author: Li Xue-cong, No. 100 Waihuan Xi Road, Guangzhou Higher Education Mega Center, Panyu District, Guangzhou, People's Republic of China Tel: 86-13922195580, 86-020-39322552

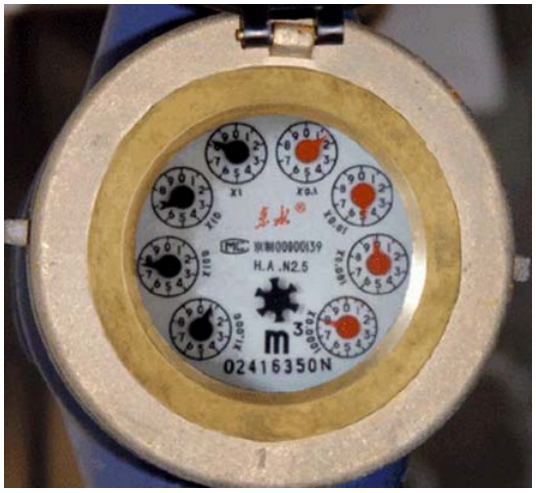

Fig. 1: The water-meter image

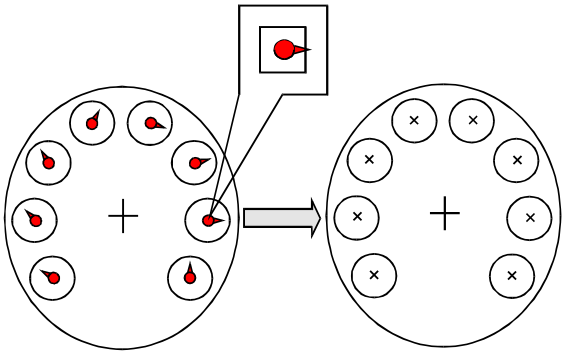

Fig. 2: Template matching

The comparability criterion used in template matching is shown as formula 1:

$$\psi = \frac{\sum_{0\le i\le m}^{0\le j\le n} S(i,j) * D(i,j)}{\sum_{0\le i\le m}^{0\le j\le n} S(i,j) * \sum_{0\le i\le m}^{0\le j\le n} D(i,j)} \quad (1)$$

where, S (i, j) denotes the gray of pixel in template image, D (i, j) denotes the gray of pixel in source image.

During the experiments, we found that pointer direction was different. To comparability criterion shown as formula 1, different pointer direction affected a little in matching operation. So, we do not take special management to solve this problem because round center need be only located roughly in this step.

Locking for round region: In this step, round region was locked completely in order to locate center coordinate accurately. Rough centers coordinates were compared

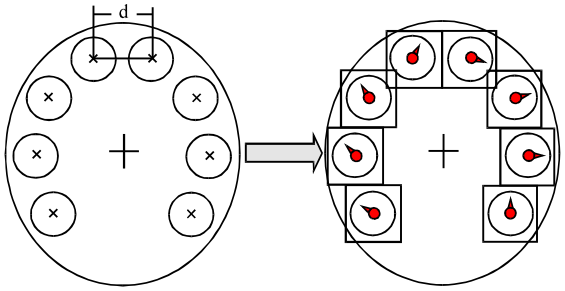

Fig. 3: Creation of square region

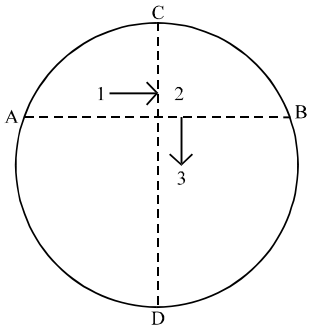

Fig. 4: Creation of square region

each other to compute the optimal square edge. The comparison is carried out like that:

$$\begin{cases} |y_p - y_q| < \alpha \\ |x_p - x_q| < \beta \end{cases}, (0 \le p, q \le N p \ne q) \quad (2)$$

where, x and y are rough coordinates, α and β are threshold, N is the total number for centers.

Substance of formula 2 is to find the two collinear rounds approximately. If there are many groups of collinear rounds, the searching will turn to find the two proximal collinear rounds. In case two such rounds were found, difference of their abscissa would be taken as the edge of square locking round region.

When square edge was confirmed, square region would be built to lock round region. The center of square region is also center of round region. This step is shown as Fig. 3.

Round edge detection and accurate location of round center: Round edge detection was implemented in every square region. So, other features outside of square region can not affect round edge detection. In this process, Canny operator was introduced. Through Gauss filtering, gradient computing, non-maximum and edge connection, single edge was detected successfully.

When round edge was ensured, round center can be located accurately. This adjusting operation is shown as Fig. 4.

In Fig. 4, position of "1" is rough round center coordinate, position of "3" is accurate round center coordinate.

First, a horizontal line was drawn across "1" position. This line intersects the round at two points named A, B. The x coordinate of round center was computed again. The computation is shown as formula 3:

$$x' = \frac{x_A + x_B}{2} \tag{3}$$

After this operation, round center was adjusted position "2". Then, a vertical line was drawn across "2" position. This line intersects the round at two points named C, D. The y coordinate of round center was computed again. The computation is shown as formula 4:

$$y' = \frac{y_A + y_B}{2} \tag{4}$$

After this operation, round center was adjusted accurate position. The coordinate of position "3" would be used in calibration.

Camera calibration: A projection model should be founded in order to complete calibration and this model also connects world coordinate and image coordinate of round center. When unknown quantities in this model were extracted, initial value of camera parameters were obtained. Let $W = [x', y', z']^T$ denote world coordinate and let $m = [u, v]^T$ denote image coordinate. And then projection relation between W and m is shown as formula 5:

$$\begin{bmatrix} u \\ v \end{bmatrix} = P \begin{bmatrix} x' \\ y' \\ z' \end{bmatrix} \tag{5}$$

where, P is a 3×4 projection matrix shown as formula 6:

$$P = A\,[R\ T] \tag{6}$$

where, R is a 3×3 rotary matrix, T is translation vector. They are both extrinsic parameters of camera. These parameters expressed position and direction of camera. A is an intrinsic parameters matrix. It is shown as formula 7:

$$A = \begin{bmatrix} f & 0 & u_0 \\ 0 & f & v_0 \\ 0 & 0 & 1 \end{bmatrix} \tag{7}$$

where, (u_0, v_0) is coordinate of image center which is the intersection between optical axis and image plane, f is camera focus which unit is pixel.

When model was founded, camera was calibrated by Zhang (2000) method.

Correction for asymmetric error: Asymmetric error consists in projection regardless what kind of shape is object. Veracity of extracting calibration datum is influenced by these errors. When angle between water-meter plane and focus plane of camera is big, circles are projected into ellipses. These changes will bring on errors during extracting round center. Using camera parameters, asymmetric error can be corrected. When asymmetric error was corrected, camera parameters would be optimized better.

In Fig. 5, focus point of camera is the origin of world coordinates. Axis z' is orthogonal to plane π_2. When circle c_2 is projected to plane π_2 through origin O, an inclined taper Λ will appear. This taper is described as formula 8:

$$(X'-\varepsilon z') + (y'-\varphi z') = \eta^2 z'^2 \tag{8}$$

where, ε and φ are gradient in x' and y' direction of Λ, η is acuity of Λ.

Point O is also the origin of camera coordinates. Axis z orthogonal to plane π_1 and axis x and axis y are parallel to axis u and axis v in image coordinates. Transform from word coordinates to camera coordinates is shown as formula 9:

$$\begin{bmatrix} x' \\ y' \\ z' \end{bmatrix} = \begin{bmatrix} a_{11} & a_{12} & a_{13} \\ a_{21} & a_{22} & a_{23} \\ a_{31} & a_{32} & a_{33} \end{bmatrix} \begin{bmatrix} x \\ y \\ z \end{bmatrix} \tag{9}$$

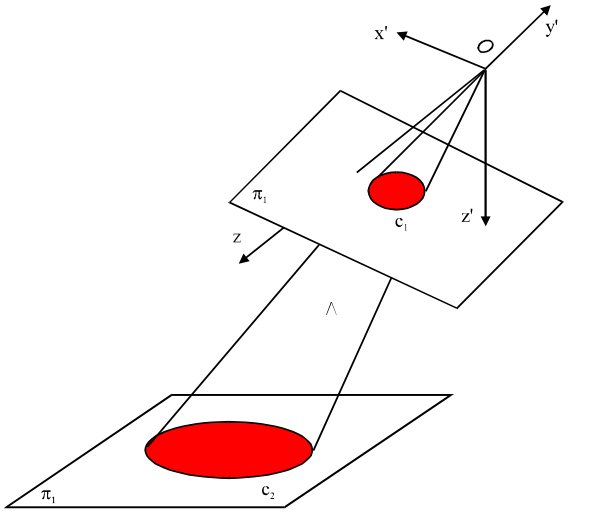

Fig. 5: Asymmetric error of round projection

where, $[a_{11}, a_{21}, a_{31}]^T$, $[a_{12}, a_{22}, a_{32}]^T$ and $[a_{13}, a_{23}, a_{33}]^T$ are a group of orthonormal units.

Take formula 8 into formula 9, the result is shown as formula 10:

$$\begin{aligned}&[(a_{11}-\varepsilon a_{31})\,x + (a_{12}-\varepsilon a_{32})\,y + (a_{13}-\varepsilon a_{33})z]^2\\ &+ [(a_{21}-\varphi a_{31})\,x + (a_{22}-\varphi a_{32})\,y + (a_{23}-\varphi a_{33}z)]^2\\ &= \eta^2\,(a_{31}x + a_{32}y + a_{33}z)^2\end{aligned} \quad (10)$$

Then, circle c_1 can be shown as formula 11:

$$(N^2 + k^2-r^2)\,x^2 + 2\,(kl + np-rs)\,x\,y + 2\,(l^2 + p^2-s^2)\,y2 + 2\,(km + nq-rt)\,x + 2\,(lm + pq-at) + m^2\,q^2-t^2 = 0 \quad (11)$$

Where:

$k = a_{11}-ta_{31}$	$n = a_{21}-sa_{31}$	$r = \eta a_{31}$
$l = a_{12}-ta_{31}$	$p = a_{32}-sa_{32}$	$s = \eta a_{32}$
$m = (a_{13}-ta_{33})f$	$q = (a_{23}-sa_{33})f$	$t = \eta a_{33}$

When λ, circle c_1 turns into ellipse. Its center $(\tilde{u}_c, \tilde{v}_c)$ can be computed by formula 12:

$$\begin{aligned}\lambda\tilde{u}_c &= (kp - nl)(lq - pm) - (ks - lr)(tl - ms) - (ns - pr)(mp - qs)\\ \lambda\tilde{v}_c &= (kp - nl)(mn - kq) - (ks - lr)(mr - kt) - (ns - pr)(qr - nt)\end{aligned} \quad (12)$$

where, λ is $(kp-nl)^2-(ks-lr)^2-(ns-pr)^2$.

When, $\eta = 0$, plane π_1 is parallel to plane π_2. Here, asymmetric error is zero. And c_1 is a circle. Its center $(\tilde{u}_0, \tilde{v}_0)$ can be computed by formula 13:

$$\begin{aligned}\tilde{u}_0 &= (lq - pm) / (kp - nl)\\ \tilde{v}_0 &= (mn - kq) / (kp - nl)\end{aligned} \quad (13)$$

In fact, $(\tilde{u}_c - \tilde{u}_0, \tilde{v}_c - \tilde{v}_0)$ is asymmetric error. Correction of them is shown as equation 14:

$$\begin{aligned}u' &= u - f(\tilde{u}_c - \tilde{u}_0)\\ v' &= v - f(\tilde{v}_c - \tilde{v}_0)\end{aligned} \quad (14)$$

When all calibration datum were corrected, accuracy of camera parameters would be improved.

EXPERIMENTAL RESULTS

In order to validate method proposed in this study, water-meter shown in Fig. 1 was calibrated. In the experiment, original image was intercepted into 400*300 pixels. After template matching, round center was roughly located. Then, round region was locked by square region. Results in these two steps are shown as Fig. 6.

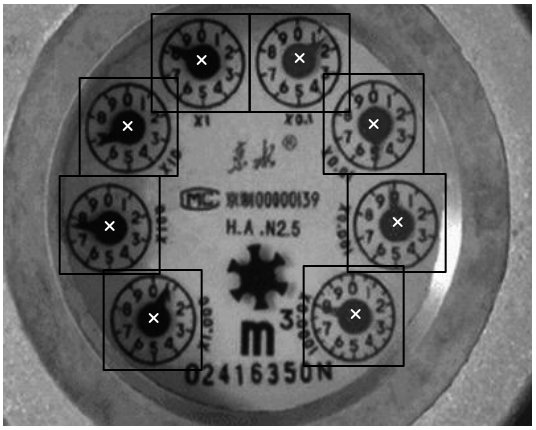

Fig. 6: Results of template matching and square region locating

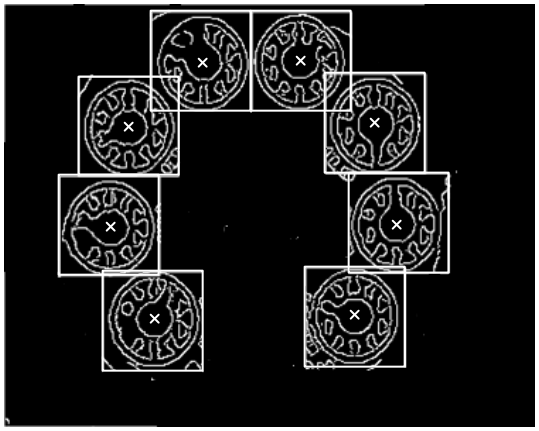

Fig. 7: Edge detection and round center adjusting

Table 1: Calibration results

Calibration item	Calibration results
f	522.363 pixels
(u_0, v_0)	(201.44 pixels, 149.16 pixels)
(k_1, k_2)	(0.33, 0.41)
(e_u, e_v)	(0.06 pixels, 0.05 pixels)

When square region was locked, pixels outside of square region were abandoned. Canny edge detection was only carried out inside of square region. Then, round center was adjusted to accurate position by using these edges. The results is shown as Fig. 7.

Using these groups of round centers, camera was calibrated by Zhang's method. The calibration results are listed in Table 1.

In Table 1, f is the camera focus, (u_0, v_0) is the coordinate of image center, (k_1, k_2) is the radial distortion, (e_u, e_v) is coordinate error after calibration.

From the results listed in Table 1, we can see that (e_u, e_v) are both under 0.1 pixels. It is obvious that calibration results are precise by using method proposed in this study.

CONCLUSIONS

Actual instance of water-meter was considered in this study. Based on that, a new camera calibration was proposed for water-meter. In this method, many image processing technologies were used such as template matching, image segmentation, Canny edge detection. Round centers were located accurately and became calibration datum. When origin camera parameters were calibrated, asymmetric error was corrected. Experimental process and results both show that method proposed in this study is practical to calibration for camera fixed on direct-reading water-meter.

ACKNOWLEDGMENT

This research was supported by the National Natural Science Foundation of China (No. 11072063, 2010-2012).

REFERENCES

Espuny, F. and J.I.B. Gil, 2011. Generic self-calibration of central cameras from two rotational flows. Int. J. Comput. Vision, 91: 131-145.

Hartley, R.I., 1999. Theory and practice of projective rectification. Int. J. Comput. Vision, 35: 115-127.

Hovany, L., 2011. The contribution of UFR in measuring water volume by water meter in a single household. Proceedings of the 3rd IEEE International Symposium on Exploitation of Renewable Energy Sources (EXPRES), March 11-12, 2011, Subotica, pp: 75-78.

Pu, Y., S. Lee and C. Kuo, 2011. Calibration of the camera used in a questionnaire input system by computer vision. Inform. Technol. J., 10: 1717-1724.

Seo, J.S., D. Blaauvv and D. Sylvester, 2011. Crosstalk-aware PWM-based on-chip links with self-calibration in 65 nm CMOS. Inst. Electr. Electron. Eng. J. Solid-State Circuits, 46: 2041-2052.

Tsai, R.Y., 1987. A versatile camera calibration technique for high-accuracy 3D machine vision metrology using off-the-shelf TV cameras and lenses. IEEE J. Robot. Autom., 3: 323-344.

Zhang, Z., 2000. A flexible new technique for camera calibration. IEEE Trans. Pattern Anal. Mach. Intell., 22: 1330-1334.

Zhao-Zheng, C. and C. Qi-Mei, 2010. Video contrast visibility detection algorithm and its implementation based on camera self-calibration. Inform. Technol. J., 32: 2907-2912.